A Physiologically Based Pharmacokinetic/Pharmacodynamic Model of the Diuretic Hydrochlorothiazide

Amanda Schwaiger and Matthias König *

Posted Date: 6 July 2026

doi: 10.20944/preprints202607.0306.v1

Keywords: digital twin; hydrochlorothiazide; hypertension; physiologically based pharmacokinetic/pharmacodynamic model (PBPK/PD); pharmacokinetics; pharmacodynamics; personalized medicine

 doi:10.20944/preprints202607.0306.v1

Article

A Physiologically Based Pharmacokinetic/Pharmacodynamic Model of the Diuretic Hydrochlorothiazide

Amanda Schwaiger [1], **and Matthias König** [2,3,*]

[1] Charité - Universitätsmedizin Berlin, Charitéplatz 1, 10117 Berlin, Germany
[2] Humboldt-Universität zu Berlin, Faculty of Life Sciences, Department of Biology, Institute of Theoretical Biology, Systems Medicine of the Liver, Unter den Linden 6, 10099 Berlin, Germany
[3] First Department of Medicine, University Hospital Schleswig-Holstein, Campus Lübeck, 23538 Lübeck, Germany
* Correspondence: koenigmx@hu-berlin.de

Abstract

Background: Hydrochlorothiazide is a widely prescribed thiazide diuretic used for the treatment of hypertension. Cardiac, hepatic, and renal impairments are common comorbidities in hypertensive patients and may contribute to substantial interindividual variability in pharmacokinetic (PK) and pharmacodynamic (PD) responses. This variability complicates dose optimization, particularly in clinically heterogeneous patient populations. **Methods**: We developed a whole-body physiologically based pharmacokinetic/pharmacodynamic (PBPK/PD) model of hydrochlorothiazide integrating oral absorption, systemic distribution, renal elimination, renal sodium, chloride, and fluid handling, and blood-pressure regulation. The model was calibrated and evaluated using systematically curated PK and PD data from 25 clinical studies in healthy individuals and patients with hypertension, cardiac impairment, hepatic impairment, or renal impairment. **Results**: Model predictions were consistent with observed dose-proportional PK and PD and captured variability in hydrochlorothiazide exposure and response across simulated comorbid conditions. Renal impairment was identified as the main driver of altered hydrochlorothiazide exposure and reduced urinary excretion. By contrast, hepatic and cardiac impairment affected PK primarily through secondary effects on renal function, rather than through direct effects on drug metabolism or absorption. **Conclusions**: The developed PBPK/PD model provides a mechanistic framework for understanding hydrochlorothiazide pharmacology across heterogeneous clinical conditions. It supports model-informed assessment of variability in exposure and response and may contribute to individualized antihypertensive therapy in patients with comorbidities.

Keywords: digital twin; hydrochlorothiazide; hypertension; physiologically based pharmacokinetic/pharmacodynamic model (PBPK/PD); pharmacokinetics; pharmacodynamics; personalized medicine

1. Introduction

Hypertension is a leading modifiable risk factor for cardiovascular morbidity and mortality and contributes substantially to the global burden of ischemic heart disease, stroke, heart failure, and chronic kidney disease. With hypertension affecting approximately 1.4 billion adults worldwide and adequate blood pressure control achieved in only 23% of patients, the need for effective, adaptable, and individualized antihypertensive treatment strategies remains pressing [1].

Hydrochlorothiazide (HCTZ) is a widely prescribed thiazide diuretic used for the treatment of hypertension. Its pharmacokinetics are well characterized. Following oral administration, HCTZ is rapidly absorbed, with an estimated absorption of 65–75%, primarily in the duodenum and proximal jejunum [2]. Absorption efficiency appears to be dose independent and generally follows first-order

 doi:10.20944/preprints202607.0306.v1

kinetics [3]. Maximum plasma concentrations are typically reached within 1–5 hours after dosing [4]. HCTZ distributes mainly within the extracellular fluid compartment and exhibits limited tissue penetration. Plasma protein binding is moderate, with reported values of approximately 40–70%, and is not considered a major determinant of variability in drug disposition [5]. The apparent volume of distribution ranges from 1.5 to 4.2 L/kg, consistent with confinement largely to extracellular water [6]. Distribution to the kidney is pronounced, whereas metabolism is minimal. HCTZ is eliminated primarily via the kidney through glomerular filtration and active tubular secretion. Under normal renal function, urinary recovery of unchanged drug typically accounts for 70–90% of the oral dose. Reported elimination half-lives range from 6 to 15 hours, and biliary excretion has been reported to account for 11.4–24.5% of elimination [2,7].

The pharmacodynamic effects of HCTZ are mediated primarily through inhibition of the Na^+/Cl^- cotransporter in the distal convoluted tubule of the nephron. The initial antihypertensive effect is generally attributed to natriuresis-induced reductions in plasma volume and, subsequently, cardiac output [8–10]. Direct vasodilatory effects have also been suggested. During chronic administration, plasma volume tends to normalize, whereas peripheral vascular resistance decreases, indicating that sustained antihypertensive efficacy may involve vascular adaptation. Modulation of neurohormonal pathways has also been proposed [11]. After oral administration, diuretic effects usually begin within approximately 2 hours, peak after about 4 hours, and persist for up to 24 hours [5]. HCTZ does not appear to lower blood pressure in normotensive individuals [12]. Despite its extensive clinical use, the mechanisms underlying its sustained antihypertensive effect remain incompletely understood.

Hypertension frequently coexists with chronic conditions that may alter both the pharmacokinetics and pharmacodynamics of antihypertensive therapy. Among these, congestive heart failure, chronic kidney disease, and chronic liver disease are particularly relevant because of their prevalence in hypertensive populations and their effects on hemodynamics, renal function, and fluid balance.

Congestive heart failure (CHF) affects an estimated 1–3% of the global population, with prevalence rising to over 7% in individuals aged 70 years or older [13]. CHF is often characterized by impaired cardiac output, neurohormonal activation, and fluid overload. Hypertension is a major risk factor for the development of CHF, and diuretics such as HCTZ are commonly prescribed to relieve fluid overload and improve blood pressure control. However, reduced cardiac output and neurohormonal activation in CHF can alter organ perfusion and thereby affect both the pharmacokinetics and diuretic efficacy of HCTZ. In patients with CHF, oral absorption of HCTZ has been reported to be approximately 50% lower than in healthy individuals, possibly due to altered intestinal wall properties or reduced splanchnic blood flow [8].

Chronic kidney disease (CKD) is present in up to 23.7% of hypertensive adults in the United States and is both a cause and a consequence of poorly controlled blood pressure [14]. More than 90% of patients with CKD have concomitant hypertension [15]. Excess extracellular fluid is considered an important contributor to both hypertension and CKD progression [15]. Renal impairment has a marked influence on HCTZ elimination: reduced glomerular filtration rate and tubular dysfunction can prolong drug half-life, increase systemic exposure, and attenuate the diuretic response because of reduced functional nephron capacity.

The interaction between cardiovascular and renal disease further complicates treatment. CHF can precipitate or aggravate renal impairment through cardiorenal syndrome, in which reduced cardiac output and increased venous congestion compromise renal perfusion and accelerate CKD progression. Patients with concomitant CHF and CKD therefore represent a particularly vulnerable subgroup with potentially altered HCTZ exposure and response.

Chronic liver disease is less directly linked to hypertension but frequently co-occurs with cardiometabolic risk factors such as obesity, diabetes, and metabolic syndrome [16]. Patients with cirrhosis or advanced hepatic impairment may develop secondary renal dysfunction, hypoalbuminemia, and altered systemic hemodynamics [17,18]. These pathophysiological changes, including hepatorenal

 doi:10.20944/preprints202607.0306.v1

interactions, may indirectly influence HCTZ pharmacokinetics and pharmacodynamics despite the minimal hepatic metabolism of the drug.

Cardiac, hepatic, and renal impairment are therefore clinically relevant in patients receiving HCTZ and may coexist within the same individual. However, dose recommendations for HCTZ in the setting of organ dysfunction remain insufficiently defined. Because the full range of comorbidity patterns cannot be comprehensively evaluated in clinical trials alone, mechanistic modeling approaches are needed to predict how organ dysfunction affects drug disposition and response and to support individualized therapy.

Previous computational modeling studies of HCTZ have addressed several specific aspects of its pharmacology, including population pharmacokinetics in healthy subjects and patients with heart failure [19], demographic effects [20], pediatric dose–exposure relationships [21], drug–drug interaction assessment using physiologically based models [22,23], and absorption kinetics [24]. Pharmacodynamic models of the antihypertensive effects of HCTZ have been developed in rats [25–27]. In humans, a combined PK/PD model has been reported as part of a drug–drug interaction study in normotensive subjects [23]. However, these models have focused on isolated aspects of HCTZ pharmacology rather than providing an integrated framework for predicting pharmacokinetics, natriuretic and antihypertensive pharmacodynamics, and organ-impairment effects across clinically relevant scenarios. In addition, existing models are limited in reproducibility because of proprietary software implementations, restricted data availability, or incomplete adherence to FAIR principles. Existing HCTZ models are systematically summarized in Supplementary Table S1, including their scope, availability, and reproducibility.

To address these limitations, we developed an open and reproducible whole-body PBPK/PD model of HCTZ encoded in SBML. The model integrates mechanistic pharmacokinetics, dose dependency, renal sodium, chloride, and fluid handling, antihypertensive pharmacodynamics, and organ dysfunction within a single framework. By providing transparent model equations, executable code, and curated clinical data, this work supports independent reuse, systematic evaluation of variability in HCTZ exposure and response, and model-informed assessment of antihypertensive therapy across clinically relevant comorbidity scenarios.

2. Materials and Methods

2.1. Systematic Literature Search and Data Curation

A systematic literature search was performed to identify clinical pharmacokinetic (PK) and pharmacodynamic (PD) data for hydrochlorothiazide (Supplementary Figure S1). The search was conducted in PubMed and PKPDAI [28] on June 12, 2024, using the search terms *hydrochlorothiazide AND pharmacokinetic* and *hydrochlorothiazide AND pharmacodynamic*. Retrieved studies were screened for single- and multiple-dose PK and PD data in healthy volunteers and in patient cohorts with renal, cardiac, or hepatic impairment.

Eligible studies were clinical studies in adults that reported clear dosing information and at least one relevant PK or PD endpoint. PK endpoints included plasma concentration–time profiles, urinary excretion data, or elimination parameters. PD endpoints included blood pressure, diuresis, or urinary electrolyte excretion. Preclinical studies, pediatric studies, reviews, and reports without sufficient PK or PD information for model development or evaluation were excluded.

Relevant data from eligible studies were curated in the open pharmacokinetics database PK-DB (https://pk-db.com) using the standardized PK-DB data format [29]. Curated study-level and subject-level information included demographics, health status, comorbidities, dosing regimens, sampling schedules, plasma concentration–time profiles, and urinary concentration or excretion profiles. Curated PD data included blood pressure, diuresis, urinary sodium and chloride excretion, angiotensin-converting enzyme (ACE) activity, renin activity, and aldosterone concentrations. Graphical data were digitized using WebPlotDigitizer [30]. Values, units, and metadata were harmonized according to the standardized PK-DB data structure [29].

 doi:10.20944/preprints202607.0306.v1

2.2. Computational Model

A whole-body physiologically based pharmacokinetic/pharmacodynamic (PBPK/PD) model of hydrochlorothiazide was developed in the Systems Biology Markup Language (SBML) [31,32] using the `sbmlutils` library [33]. The model consists of linked submodels representing intestinal absorption, systemic distribution, renal and intestinal elimination, kidney function, hepatic function, and blood pressure regulation. The framework further includes pharmacodynamic components describing renal sodium, chloride, and fluid handling, as well as systemic blood pressure regulation.

Simulations were performed with `sbmlsim` [34] and `libRoadRunner` [35,36]. Model visualizations were generated with `cy3sbml` [37,38]. The complete model, including simulation scripts and documentation, is available in SBML format under a CC-BY 4.0 license via GitHub (https://github.com/matthiaskoenig/hctz-model) and is archived on Zenodo as version 0.7.0 (https://doi.org/10.5281/zenodo.20409640) [39].

Cardiac impairment was implemented using the parameter `f_cardiac_function`, where a value of 1.0 represents normal cardiac function, corresponding to a cardiac output of approximately 4.5–6 L/min. Simulated impairment levels were scaled to represent mild, moderate, and severe reductions in cardiac output, with parameter values of 0.75, 0.50, and 0.25, respectively. This adjustment affected systemic hemodynamics, renal perfusion, and downstream clearance processes, thereby capturing the impact of congestive heart failure on hydrochlorothiazide disposition.

Renal impairment was represented by scaling renal function through the parameter `KI__f_renal_function`, with a value of 1.0 indicating normal kidney function, corresponding to a glomerular filtration rate of approximately 101 mL/min. Progressive renal impairment was simulated using values of 0.69, 0.32, and 0.19 for mild, moderate, and severe impairment, respectively. These values reflect reduced glomerular filtration rates consistent with clinical chronic kidney disease staging: 69.5 mL/min/1.73 m^2 for mild, 32.5 mL/min/1.73 m^2 for moderate, and 19.5 mL/min/1.73 m^2 for severe renal dysfunction [40].

Hepatic impairment was implemented using the parameter `f_cirrhosis`, with a value of 0.0 representing normal hepatic function and increasing values representing progressive cirrhotic impairment. Impairment levels were scaled according to Child–Pugh classifications, corresponding to mild, moderate, and severe impairment, with parameter values of 0.40, 0.70, and 0.81, respectively [41]. Although hydrochlorothiazide undergoes minimal hepatic metabolism, hepatic impairment was included to capture secondary effects such as altered systemic hemodynamic changes and renal perfusion. These mechanisms may indirectly influence hydrochlorothiazide disposition and diuretic response in patients with cirrhosis or advanced liver disease.

2.3. Parameter Optimization

Pharmacokinetic (PK) and pharmacodynamic (PD) parameters were optimized using the curated clinical datasets. For the PK model, the optimized parameters comprised the tissue distribution factor (`ftissue_hctz`), the tissue-to-plasma partition coefficient (`Kp_hctz`), the dissolution rate (`Ka_dis_hctz`), the intestinal absorption rate constant (`GU__HCTZABS_k`), the maximum urinary excretion rate (`KI__HCTZEX_Vmax`), and the Michaelis constant for urinary excretion (`KI__HCTZEX_Km`). For the PD model, optimization targeted sodium chloride intake from food (`vin_nacl`) and the EC_{50} values for hydrochlorothiazide-induced urinary sodium, chloride, and water excretion (`E50_hctz_na`, `E50_hctz_cl`, and `E50_hctz_h2o`, respectively). Optimization was performed across multiple dose levels and under fed and fasted conditions. Multiple local optimization runs were applied sequentially, with PK parameters estimated first and PD parameters estimated subsequently.

Optimized parameter values and optimization diagnostics are reported in Supplementary Section S3, including fitted PK and PD parameter sets, convergence behavior, and goodness-of-fit assessments for both model components.

The objective function, defined as a function of the parameter vector $\vec{p}$, minimized the sum of squared weighted residuals $r_{i,k}$ across all time courses k and data points i. Time courses were weighted according to the number of participants in each study, n_k, and individual data points were weighted

 doi:10.20944/preprints202607.0306.v1

by the inverse of the associated measurement uncertainty, represented by the standard deviation $\sigma_{i,k}$. This resulted in weights $w_{i,k} = n_k/\sigma_{i,k}$:

$$F(\vec{p}) = \frac{1}{2}\sum_{i,k}(w_{i,k} \cdot r_{i,k}(\vec{p}))^2.$$

Accordingly, data points with lower measurement uncertainty and time courses from studies with larger sample sizes contributed more strongly to the objective function.

Multiple optimization runs ($n = 100$) were performed using different initial parameter values to reduce sensitivity to local minima. Optimization was conducted sequentially: PK parameters were estimated first, followed by PD parameters.

2.4. Simulations

For each curated clinical study (Table 1), a corresponding *in silico* experiment was implemented to reproduce the reported dosing regimen and study conditions. Study-specific parameters, including route of administration, dose, dosing schedule, baseline blood pressure, and hepatic, cardiac, and renal function, were adjusted according to the information reported in each study. Multiple-dose protocols were implemented where applicable.

To further investigate sources of variability, additional simulation experiments and parameter scans were performed across physiologically relevant ranges of hepatic, cardiac, and renal function, as well as dose. These simulations enabled systematic evaluation of the effects of key physiological and pathophysiological parameters on pharmacokinetic and pharmacodynamic outcomes.

2.5. Pharmacokinetic and Pharmacodynamic Parameters

Pharmacokinetic parameters of hydrochlorothiazide were derived from simulated plasma concentration–time profiles and urinary excretion profiles using standard non-compartmental analysis. Pharmacodynamic outcomes were evaluated based on simulated urinary sodium and chloride excretion, diuresis, and blood pressure responses. Blood pressure simulations incorporated study-specific baseline blood pressure values where available.

Simulated concentration–time profiles, urinary excretion profiles, pharmacodynamic response profiles, and derived pharmacokinetic and pharmacodynamic parameters were compared with the curated clinical data.

3. Results

3.1. Hydrochlorothiazide Database

A total of 25 clinical studies met the inclusion criteria and were systematically curated for PBPK/PD model development and evaluation. The curated studies covered diverse study populations, dosing regimens, routes of administration, and clinical conditions, including healthy individuals and patients with hypertension, renal impairment, cardiac impairment, or hepatic impairment. The study identification, screening, and inclusion workflow is shown in Supplementary Figure S1. An overview of the curated studies and their key data characteristics is provided in Table 1.

The curated data were integrated into an open hydrochlorothiazide pharmacokinetic/ pharmacodynamic database. Each study was assigned a unique PK-DB identifier linked to the corresponding curated dataset in the publicly available PK-DB resource. The database includes study-level metadata, dosing regimens, demographic and clinical information, pharmacokinetic concentration–time and urinary excretion data, and pharmacodynamic endpoints, including blood pressure, diuresis, and urinary sodium and chloride excretion.

3.2. Computational Model

A whole-body physiologically based pharmacokinetic/pharmacodynamic (PBPK/PD) model of hydrochlorothiazide was developed (see Figure 1). The model comprises the key organs and

 doi:10.20944/preprints202607.0306.v1

functional units involved in hydrochlorothiazide pharmacokinetics and pharmacodynamics, including the gastrointestinal tract, liver, kidneys, nephron, body-fluid compartments, and blood pressure regulation, all connected through the systemic circulation. The model incorporates physiological and pathophysiological factors relevant to hydrochlorothiazide exposure and response, including administered dose, renal impairment represented by glomerular filtration rate, hepatic impairment represented by the degree of cirrhosis according to Child–Pugh classification, and cardiac impairment represented by cardiac output.

Model parameters were optimized against a subset of the curated clinical dataset. The optimized model showed good agreement between simulations and observed data across different patient populations and dosing scenarios. This framework enables systematic exploration of dosing regimens and common comorbidities affecting hydrochlorothiazide exposure and response, thereby providing a basis for model-informed assessment of individualized dosing strategies.

The intestinal submodel describes dissolution, absorption, transport, and gastrointestinal excretion of hydrochlorothiazide. It is structured into five compartments: stomach, intestinal lumen, enterocytes, blood plasma, and feces. Hydrochlorothiazide dissolves in the stomach and is subsequently transferred through the intestinal lumen and enterocytes into the systemic circulation.

The kidney model describes renal elimination of hydrochlorothiazide from plasma into urine. As shown in Figure 1, the kidney model includes plasma and urine compartments, with renal clearance represented as unidirectional transport from plasma to urine. A nephron submodel was integrated to simulate sodium, chloride, and water transport in the early distal tubule, the primary site of hydrochlorothiazide action.

Body-fluid compartments were included to describe the pharmacodynamic effects of hydrochlorothiazide on diuresis and blood pressure. The fluid model is coupled to the kidney and nephron submodels and links drug-induced changes in renal sodium, chloride, and water handling to systemic fluid balance and blood pressure regulation.

After establishing the PBPK/PD model structure, selected model parameters were optimized using a subset of the curated clinical data. Pharmacokinetic parameters were optimized first, followed by pharmacodynamic parameters. Optimization diagnostics, including convergence behavior and goodness-of-fit assessments, are provided in Supplementary Section S3.

3.3. Dose Dependency

Oral hydrochlorothiazide doses ranging from 5 to 200 mg and intravenous doses ranging from 1 to 35 mg were simulated. The model reproduced dose-dependent pharmacokinetic and pharmacodynamic behavior across the simulated dose range, as shown in Figures 2 and 3. Simulated hydrochlorothiazide concentrations in plasma, urine, and feces increased with dose and were consistent with the general trends observed in clinical data from single- and multiple-dose studies.

The model captured the observed dose dependency reported by Azumaya1990, Jordo1979, Patel1984, and Beermann1976 [2,7,42,43]. Simulated C_{max} and $AUC_{0-\infty}$ increased more than proportionally with dose, whereas the apparent elimination half-life and renal elimination rate decreased with increasing dose. These patterns indicate nonlinear pharmacokinetics over the investigated dose range.

Pharmacodynamic responses also increased with dose. Higher doses resulted in greater maximum diuresis, reaching up to 270 mL/h after a 100 mg dose, as well as increased urinary sodium and chloride excretion. Higher doses were also associated with stronger reductions in systolic and diastolic blood pressure, reaching values of approximately 109 and 73 mmHg, respectively, in the simulations. Overall, the simulated dose-dependent pharmacokinetic and pharmacodynamic trends were consistent with the curated clinical data.

3.4. Hepatic Impairment

Simulations of different degrees of liver cirrhosis were performed to investigate the effects of hepatic impairment on hydrochlorothiazide pharmacokinetics and pharmacodynamics. As shown in Supplementary Figure S46, changes in hepatic function had only minor effects on simulated

 doi:10.20944/preprints202607.0306.v1

hydrochlorothiazide concentrations in plasma, urine, and feces. This finding is consistent with the minimal hepatic metabolism of hydrochlorothiazide.

With increasing cirrhosis severity, simulated $AUC_{0-\infty}$ increased, whereas the apparent elimination half-life ($t_{1/2}$) showed only minor changes. Overall, hepatic impairment had limited direct effects on hydrochlorothiazide exposure, and the simulated pharmacokinetic profiles were consistent with the general trends observed in the curated clinical data.

3.5. Cardiac Impairment

Different levels of cardiac output, ranging from 0 to 6 L/min, were simulated to investigate the effects of cardiac impairment on hydrochlorothiazide pharmacokinetics. As shown in Figure 4, changes in cardiac output had only minor effects on simulated hydrochlorothiazide concentrations in plasma, urine, and feces. Fecal hydrochlorothiazide concentrations were largely unchanged across the simulated range of cardiac output.

Simulated $AUC_{0-\infty}$ and apparent elimination half-life ($t_{1/2}$) changed moderately with increasing cardiac impairment. However, the magnitude of these effects was substantially smaller than that observed for renal impairment, indicating that cardiac impairment alone is not a major determinant of hydrochlorothiazide exposure in the model. The moderate changes in pharmacokinetic parameters were primarily attributable to cardiac-output-dependent changes in glomerular filtration rate, which indirectly affected renal elimination.

Overall, the simulated pharmacokinetic profiles were consistent with the general trends observed in the curated clinical data. In contrast to the interpretation proposed by Beermann et al. [8], the model suggests that reduced cardiac output alone does not substantially alter hydrochlorothiazide exposure. The previously reported differences in patients with congestive heart failure may therefore reflect secondary effects, such as altered renal function, changes in intestinal absorption, or other disease-related physiological changes, rather than cardiac impairment alone.

3.6. Renal Impairment

Simulations across different levels of renal function, ranging from 0.1 to 1.0 and corresponding to an eGFR range from less than 30 to more than 90 mL/min/1.73 m^2, were performed to investigate the effects of renal impairment on hydrochlorothiazide pharmacokinetics and pharmacodynamics. As shown in Figure 5, reduced renal function resulted in higher simulated hydrochlorothiazide plasma concentrations and reduced urinary excretion, whereas fecal hydrochlorothiazide concentrations remained largely unchanged. These findings highlight the central role of renal elimination in hydrochlorothiazide disposition.

Simulated $AUC_{0-\infty}$ and apparent elimination half-life ($t_{1/2}$) increased with decreasing renal function, consistent with impaired renal clearance. The magnitude of these changes was substantially larger than that observed for hepatic or cardiac impairment, indicating that renal function is the primary determinant of hydrochlorothiazide exposure in the model. Simulated pharmacokinetic and pharmacodynamic profiles were consistent with the general trends observed in the curated clinical data.

Table 1. Overview of included studies. All 25 studies included are listed with key identifiers (Study, PK-DB ID), dosing regimen, dose, route and participant characteristics: healthy, hypertension (HTN), cardiac impairment (CI), renal impairment (RI), and hepatic impairment (HI). Pharmacokinetic data include plasma concentrations (Plasma), urinary recovery (Urine) and fecal recovery (Feces); pharmacodynamic data include blood pressure (BP), diuresis (Diu), urinary sodium excretion (Na), and urinary chloride excretion (Cl) .

Study	PK-DB	Dosing	Dose [mg]	Route	Healthy	HTN	CI	RI	HI	Plasma	Urine	Feces	BP	Diuresis	Na	Cl
Anderson1961 [44]	PKDB01102	single	50	p.o., i.v.	✓		✓	✓	✓	✓	✓					
Azumaya1990 [42]	PKDB01103	single	12.5, 25	p.o.	✓					✓						
Barbhaiya1982 [3]	PKDB00751	single	50	p.o.	✓					✓	✓					
Barbhaiya1982a [45]	PKDB01104	single	50	p.o.	✓					✓	✓					
Beermann1976 [2]	PKDB00752	single	5, 50, 75 (p.o.) 1, 35 (i.v.)	p.o., i.v.	✓	✓				✓	✓	✓				
Beermann1977a [46]	PKDB00821	single	12.5, 25, 50, 75	p.o.	✓					✓	✓			✓	✓	✓
Beermann1979 [8]	PKDB01105	single	50, 75	p.o.			✓	✓		✓	✓					
Devineni2014 [47]	PKDB00879	multiple	25	p.o.	✓					✓						
Giudicelli1987 [48]	PKDB00753	single, multiple	25	p.o.		✓				✓						
Heise2015 [49]	PKDB00852	multiple	25	p.o.						✓	✓					
Howes1991 [50]	PKDB00777	single	25	p.o.	✓					✓	✓		✓			
Hsiao2015 [51]	PKDB00754	multiple	25	p.o.	✓					✓						
Hunninghake1986 [52]	PKDB00755	single	75	p.o.	✓					✓	✓					
Jeon2012 [53]	PKDB00756	multiple	25	p.o.	✓					✓	✓		✓	✓		
Jordo1979 [43]	PKDB00757	single	12.5, 25	p.o.	✓					✓	✓					
Knauf1995 [54]	PKDB????	single	25, 50	p.o.	✓			✓							✓	✓
Koytchev2004 [55]	PKDB00853	single	12.5	p.o.	✓					✓						
Niemeyer1983 [56]	PKDB00758	single	50	p.o.	✓	✓		✓		✓	✓					
Nilsen1989 [57]	PKDB01107	single	25	p.o.	✓	✓					✓		✓		✓	
Niopas2004 [58]	PKDB00789	single	12.5	p.o.	✓					✓						
Patel1984 [7]	PKDB00759	single	25, 50, 100, 200	p.o.	✓					✓	✓				✓	✓
Ripley2000 [59]	PKDB01108	single	25	p.o.		✓					✓				✓	
Vaidyanathan2006 [60]	PKDB00681	multiple	25	p.o.	✓					✓						
Weir1998 [61]	PKDB00760	multiple	25	p.o.	✓					✓	✓					
Williams1982 [62]	PKDB01109	single	50, 100	p.o.	✓					✓	✓			✓	✓	✓

 doi:10.20944/preprints202607.0306.v1

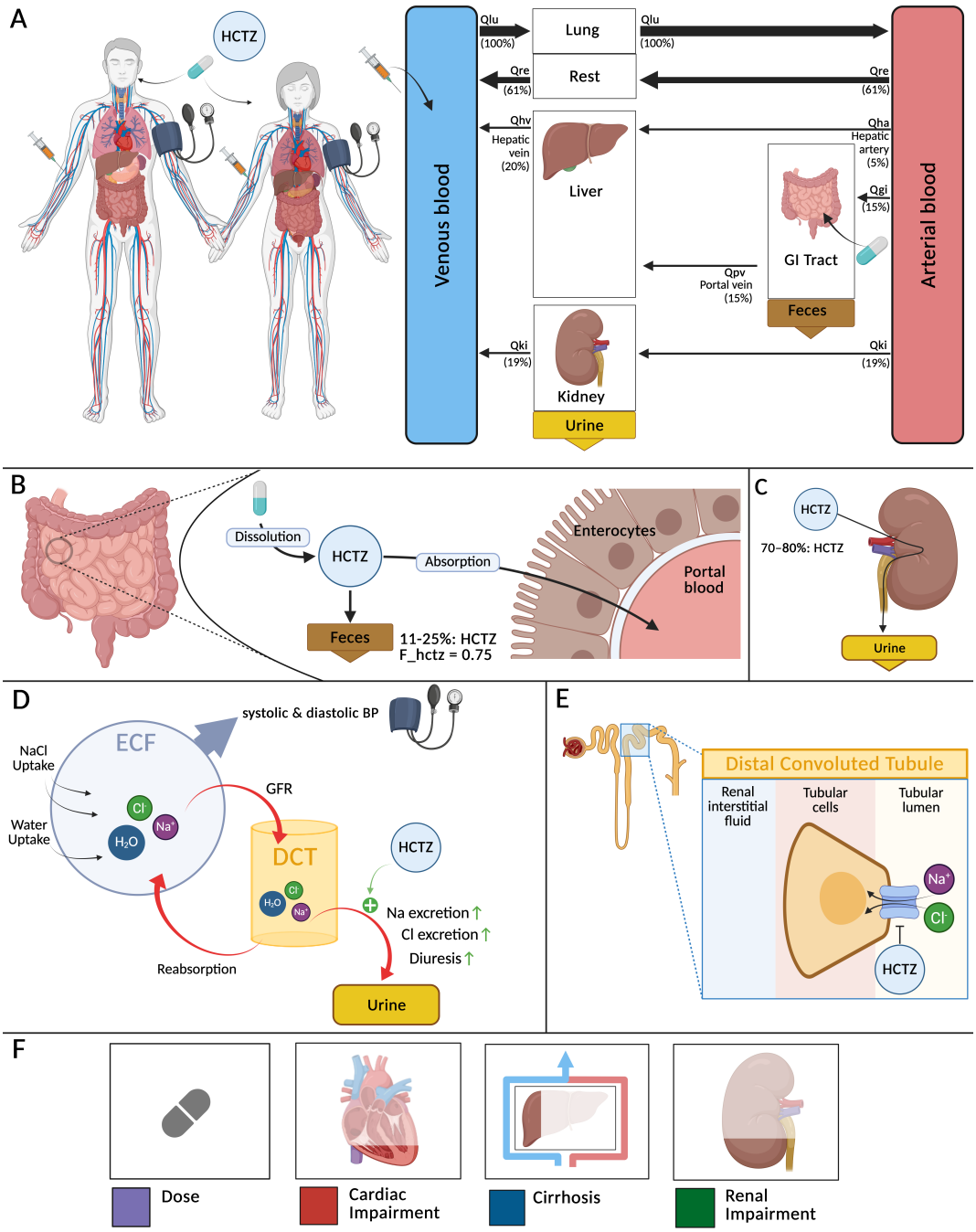

Figure 1. Physiologically based pharmacokinetic/pharmacodynamic (PBPK/PD) model of hydrochlorothiazide. **A)** Whole-body model illustrating oral and intravenous administration of hydrochlorothiazide (HCTZ), its distribution via systemic circulation, and the key organs involved in its absorption, metabolism, and elimination, including the gastrointestinal tract liver and kidneys. **B)** Gastrointestinal model depicting the absorption of HCTZ and showing minimal role of intestinal excretion. **C)** Kidney model emphasizing renal excretion as the principal elimination route of HCTZ ensuring that the fraction of drug reaching the tubular site of action is appropriately represented. **D)** Fluid model linking HCTZ mechanism of action to blood pressure as a function of extracellular fluid. Sodium and chloride, followed by water, move from the ECF via glomerular filtration to the tubular lumen illustrated as the distal convoluted tubule (DCT) to then be excreted in the urine. HCTZ increases sodium and chloride excretion, thereby increasing diuresis. ECF volume reduction decreases systolic and diastolic blood pressure. **E)** HCTZ mechanism of action in the early distal convoluted tubule as part of the kidney model: inhibition of sodium-chloride co-transporter, thereby reducing sodium and chloride reabsorption. **F)** Factors affecting PK and PD profiles accounted for in the model: administered dose, hepatic impairment (cirrhosis), cardiac impairment, and renal impairment.

 doi:10.20944/preprints202607.0306.v1

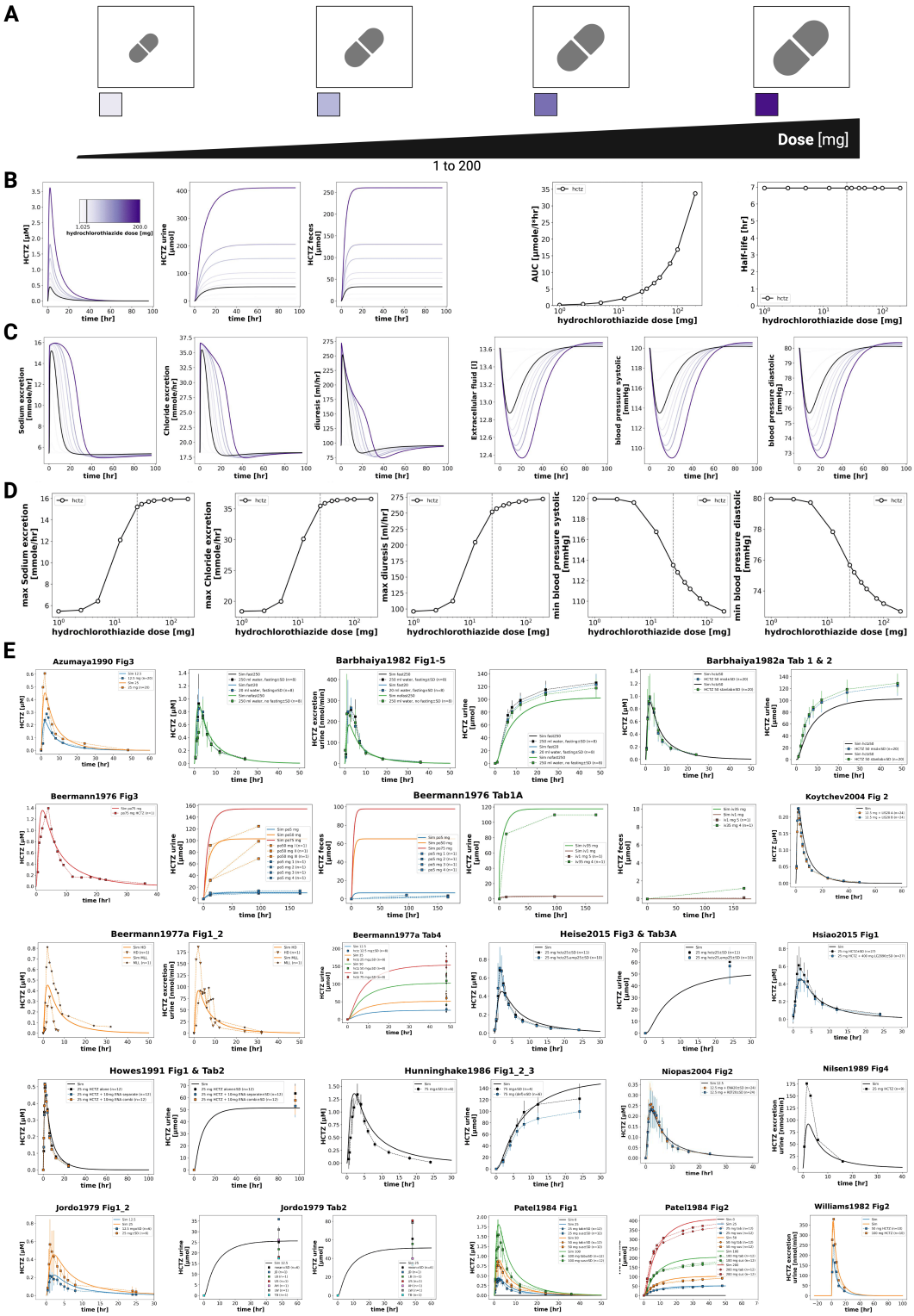

Figure 2. Dose-dependent pharmacokinetics and pharmacodynamics of hydrochlorothiazide. A) Oral and intravenous dose range (1–200 mg) evaluated in the simulations. **B)** Simulated PK time-courses for various doses and dose dependency relationships for key PK parameters. Correlation between HCTZ dose and key pharmacokinetic parameters is illustrated for $AUC_{0-\mathrm{inf}}$ and $t_{1/2}$. **C)** Simulated PD time-courses for various doses and dose dependency relationships for key PD parameters. **D)** Correlation between HCTZ dose and key pharmacodynamic parameters is illustrated. **E)** Simulated (solid lines) versus observed (dashed lines/symbols) plasma and urine concentration-time profiles of hydrochlorothiazide across various single oral doses in clinical studies. Observed data are presented as mean or mean ± SD where available. Data from Azumaya1990 [42], Barbhaiya1982 [3], Barbhaiya1982a [45], Beermann1976 [2], Beermann1977a [46], Heise2015 [49], Howes1991 [50], Hsiao2015 [51], Hunninghake1986 [52], Jordo1979 [43], Koytchev2004 [63], Nilsen1989 [57], Niopas2011 [58], Patel1984 [7], and Williams1982 [62].

 doi:10.20944/preprints202607.0306.v1

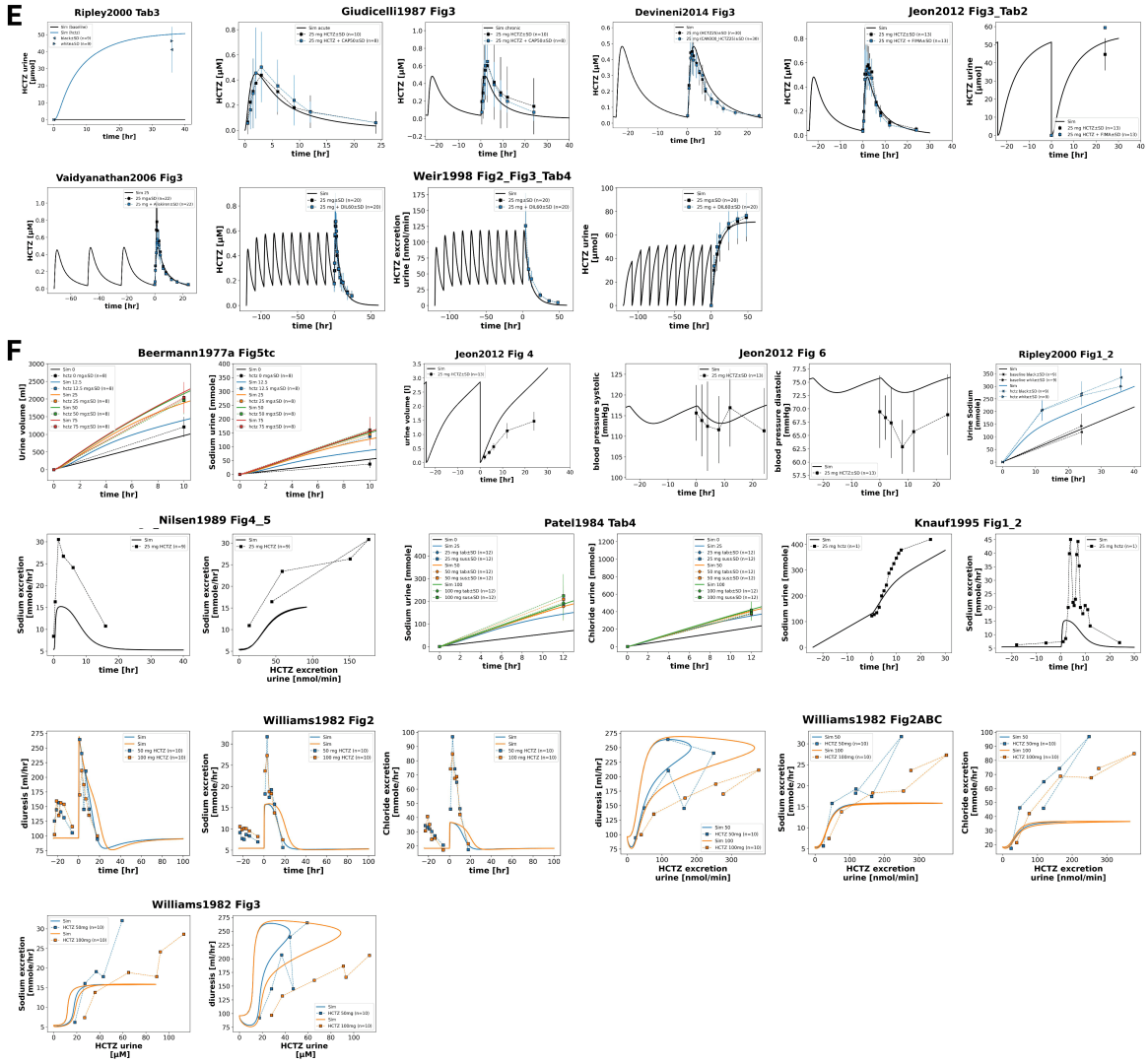

Figure 3. Additional dose-dependent clinical studies of hydrochlorothiazide. E continued) Simulated (solid lines) versus observed (symbols with dashed lines) plasma and urine concentration-time profiles of hydrochlorothiazide across single oral doses and various multiple oral doses in clinical studies. Data from Ripley2000 [59], Giudicelli1987 [48], Devineni2014 [47], Jeon2012 [53], Vaidyanathan2006 [60], and Weir1998 [61]. **F)** Simulated (solid lines) versus observed (dashed lines/symbols) pharmacodynamic profiles of hydrochlorothiazide across various oral doses in clinical studies. Observed data are presented as mean or mean ± SD where available. Data from Beermann1977a [46], Jeon2012 [53], Ripley2000 [59], Nilsen1989 [57], Patel1984 [7], Knauf1995 [54] and Williams1982 [62].

 doi:10.20944/preprints202607.0306.v1

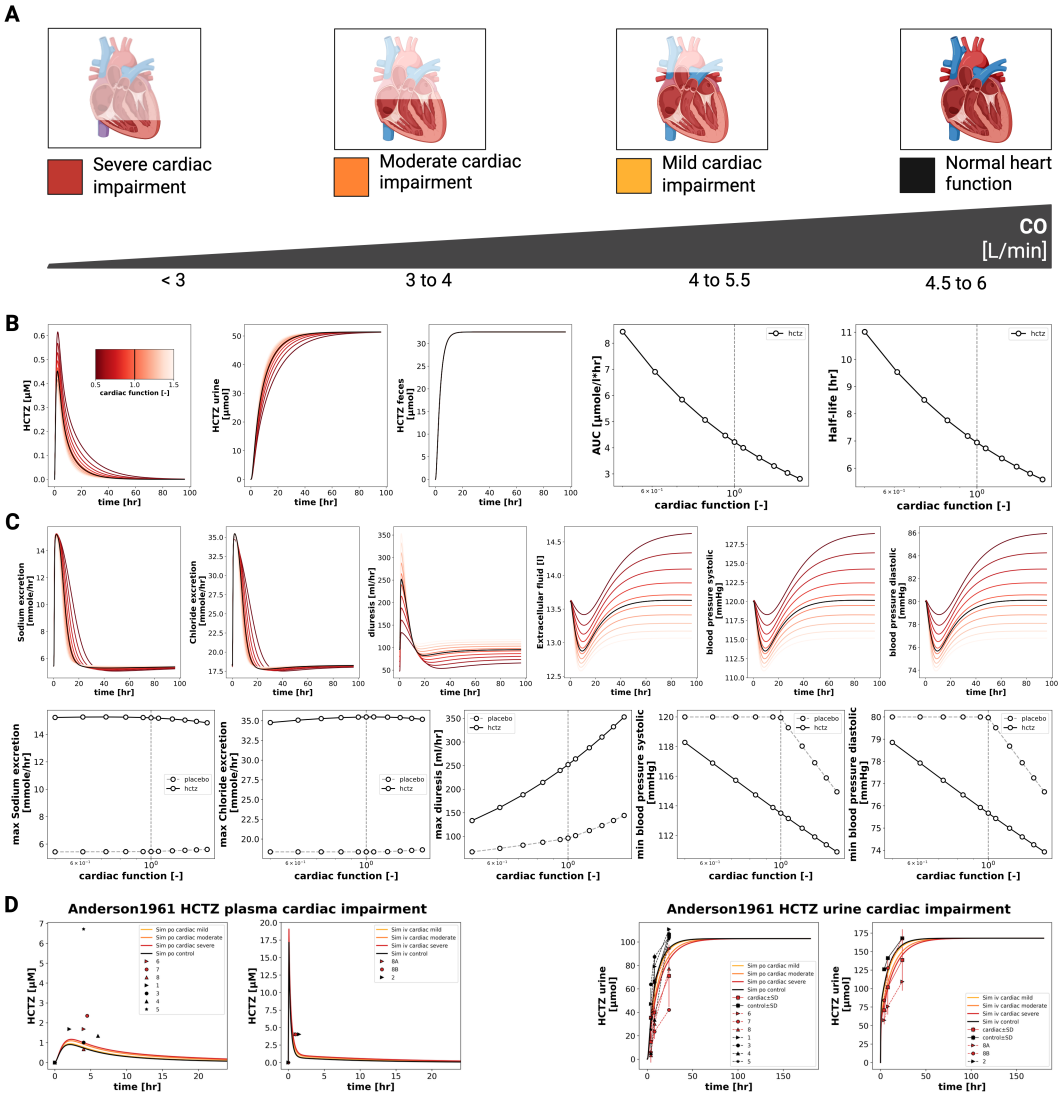

Figure 4. Effects of cardiac impairment on the pharmacokinetics and pharmacodynamics of hydrochlorothiazide. A) Classification of heart function levels based on cardiac output, distinguishing normal function from mild, moderate, and severe cardiac impairment. **B)** Simulated pharmacokinetic time-course profiles across increasing degrees of cardiac impairment. Correlation between cardiac function and key pharmacokinetic parameters is illustrated for $AUC_{0-\text{inf}}$ and $t_{1/2}$. **C)** Simulated pharmacodynamic time-course profiles across increasing degrees of cardiac impairment. Correlation between cardiac function and key pharmacodynamic parameters is illustrated. **D)** Comparison of simulated (solid lines) and observed data (dashed lines/symbols) for plasma concentration-time profiles and cumulative urinary excretion in patients with cardiac impairment from Anderson1961 [44].

 doi:10.20944/preprints202607.0306.v1

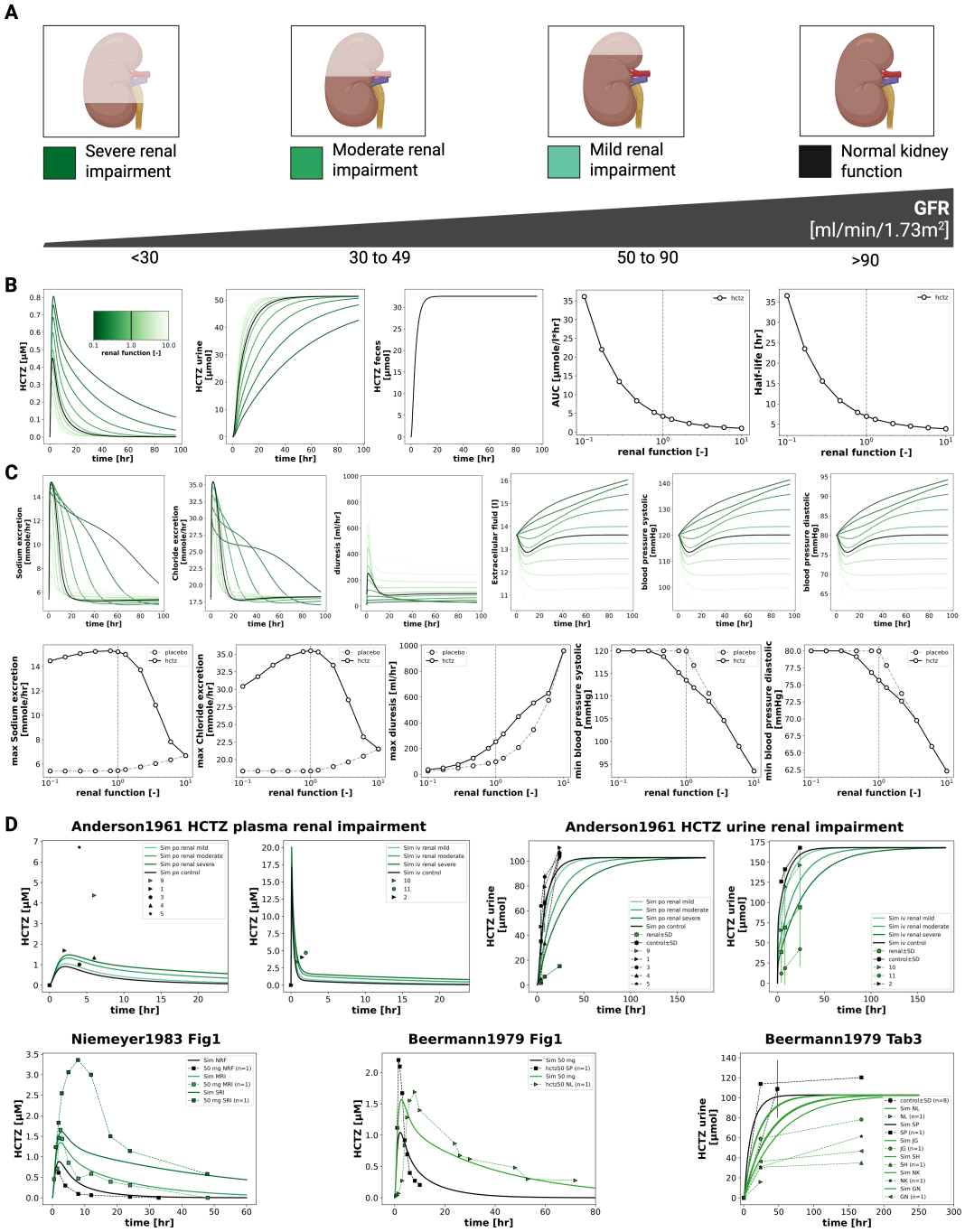

Figure 5. Effects of renal impairment on the pharmacokinetics and pharmacodynamics of hydrochlorothiazide. **A)** Classification of renal function levels based on estimated glomerular filtration rate (eGFR), distinguishing normal function from mild, moderate, and severe renal impairment. **B)** Simulated pharmacokinetic time-course profiles across graded renal function levels. Correlation between renal function and key pharmacokinetic parameters is illustrated for $AUC_{0-\inf}$ and $t_{1/2}$. **C)** Simulated pharmacodynamic time-course profiles across graded renal function levels. Correlation between renal function and key pharmacodynamic parameters is illustrated. **D)** Comparison of simulated (solid lines) and observed data (dashed lines/symbols) for plasma concentration-time profiles and cumulative urinary excretion across renal function levels in selected studies: Anderson1961 [44], Niemeyer1983 [56], and Beermann1979 [8].

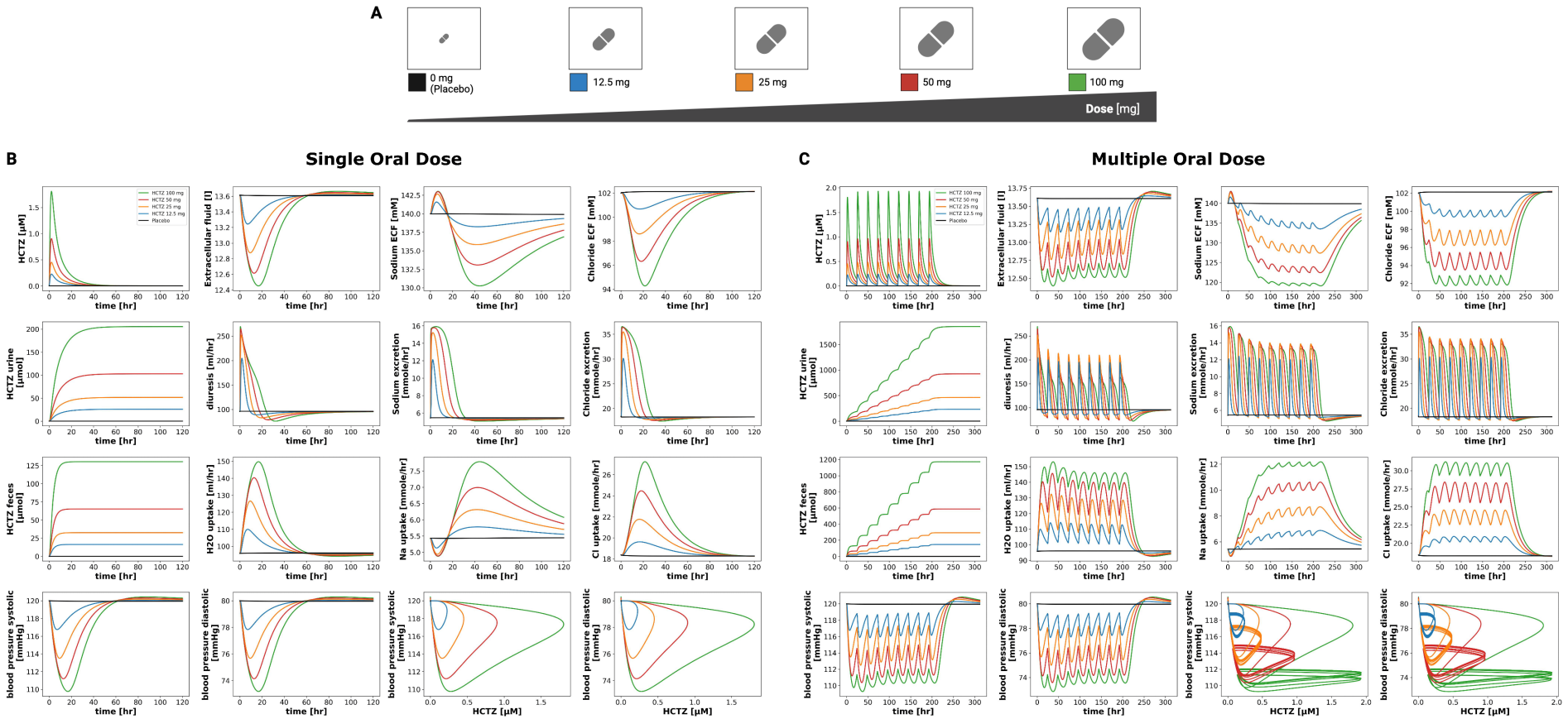

Figure 6. PBPK/PD HCTZ model simulating single and multiple oral dose administration of hydrochlorothiazide showing dose-dependent pharmacokinetics and pharmacodynamics. A) Oral doses (0–100 mg) shown in the simulations. **B & C)** For single (B) and multiple (C) oral dose administration, simulated PK and PD time-courses and dose dependency relationships for all key parameters: plasma concentration (HCTZ), amount in urine (HCTZ urine) and feces (HCTZ feces), extracellular fluid volume (ECF), sodium and chloride concentration in ECF, diuresis, sodium and chloride excretion, water uptake, sodium and chloride uptake, as well as systolic and diastolic blood pressure. Lastly, the correlations between HCTZ plasma concentration and blood pressure are illustrated.

 doi:10.20944/preprints202607.0306.v1

4. Discussion

In this study, we compiled a curated clinical dataset of hydrochlorothiazide pharmacokinetics and pharmacodynamics from 25 studies and used it to develop a whole-body PBPK/PD model. The dataset included healthy and hypertensive individuals as well as patients with renal, hepatic, or cardiac impairment. Plasma concentration–time profiles and cumulative urinary excretion were consistently reported across studies, whereas pharmacodynamic endpoints were available for a subset of studies and were used to calibrate the exposure–response relationship.

The model integrates oral absorption, systemic distribution, predominantly renal elimination, renal sodium and water handling, and blood pressure regulation. Simulations showed good agreement with observed pharmacokinetic data across therapeutic doses and organ-function strata. Dose-dependent exposure and diuretic effects were reproduced within the clinical range. Renal impairment was identified as the main determinant of altered hydrochlorothiazide exposure and urinary excretion, whereas hepatic and cardiac impairment affected pharmacokinetics primarily through secondary effects on renal function. Overall, the model provides a mechanistic framework to characterize hydrochlorothiazide PK/PD variability across clinically relevant conditions.

Although hydrochlorothiazide undergoes minimal hepatic metabolism, the curated data and simulations indicate that hepatic impairment may indirectly influence hydrochlorothiazide pharmacokinetics. In subjects with hepatic impairment, reduced peak plasma concentrations and urinary excretion were observed in some datasets. These findings suggest that hepatic dysfunction may affect hydrochlorothiazide disposition through mechanisms other than metabolism. In advanced liver disease, impaired hepatic function is often accompanied by cirrhosis-associated systemic hemodynamic changes, including reduced effective arterial blood volume, splanchnic vasodilation, and secondary renal hypoperfusion. These alterations are characteristic of hepatorenal physiology and may reduce renal drug clearance or alter drug delivery to the kidney.

Renal dysfunction is common in patients with chronic liver disease. The incidence of acute renal dysfunction in hospitalized patients with chronic liver disease has been reported to be approximately 20% [64], and patients with chronic liver disease are at increased risk of acute kidney injury [65]. Such pathophysiological changes may impair renal elimination and reduce urinary recovery of hydrochlorothiazide. In addition, hypoalbuminemia associated with cirrhosis may alter plasma protein binding and distribution, although hydrochlorothiazide protein binding is only moderate (and protein binding was not included in the model). Together, these mechanisms suggest that hepatic impairment may influence hydrochlorothiazide pharmacokinetics indirectly, particularly in patients with advanced cirrhosis or concomitant renal dysfunction.

Reduced hydrochlorothiazide absorption in cardiac failure has previously been attributed to alterations in intestinal wall properties or reduced splanchnic blood flow [8]. However, closer examination of the available patient-level data does not provide clear support for a direct effect of cardiac impairment alone on hydrochlorothiazide absorption. In the study by Beermann1979, all participants were diagnosed with cardiac failure, yet only one patient (SP) had preserved renal function, as indicated by normal creatinine clearance. This patient showed urinary recovery of hydrochlorothiazide comparable to that observed in individuals without cardiac disease, despite the presence of cardiac failure. In contrast, reduced cumulative urinary recovery was observed mainly in patients with impaired renal function. These findings suggest that reduced hydrochlorothiazide recovery in cardiac failure may be more closely related to renal dysfunction than to cardiac impairment per se.

Anderson1961 similarly proposed that impaired gastrointestinal absorption in patients with heart failure may contribute to reduced hydrochlorothiazide recovery but is unlikely to be the sole explanatory factor [44]. Changes in renal hemodynamics associated with congestive heart failure, as well as alterations in body fluid and electrolyte status, may also contribute to altered renal excretion. Consistent with this interpretation, our simulations suggest that reduced cardiac output alone has only limited effects on hydrochlorothiazide exposure, whereas secondary changes in renal function can modestly influence pharmacokinetic parameters.

 doi:10.20944/preprints202607.0306.v1

The PBPK/PD model confirmed that renal impairment predominantly affects hydrochlorothiazide clearance. With decreasing renal function, simulated plasma concentrations and systemic exposure increased, whereas urinary excretion was reduced. This pattern is consistent with the known elimination pathway of hydrochlorothiazide, which is predominantly excreted unchanged via the kidneys. Accumulation of hydrochlorothiazide in renal impairment may contribute to augmented or prolonged diuretic and antihypertensive effects, but may also increase the risk of excessive volume depletion or electrolyte disturbances. Careful monitoring of therapeutic response, renal function, volume status, and electrolyte balance is therefore particularly important in patients with impaired renal function.

Anderson reported different degrees of reduced urinary hydrochlorothiazide excretion in patients with renal impairment [44]. However, creatinine clearance and glomerular filtration rate were not reported for these patients, limiting direct interpretation of the observed variability. Model-based comparison suggests that patient 11 may have had severe renal impairment, whereas patient 10 may have had moderate renal impairment. These examples illustrate how mechanistic PBPK/PD modeling can support interpretation of historical clinical data when key physiological covariates were incompletely reported.

The role of hydrochlorothiazide and other thiazide or thiazide-like diuretics in chronic kidney disease is being re-evaluated. Traditional teaching suggested that thiazide diuretics become ineffective once eGFR falls below approximately 30 mL/min/1.73 m^2. However, clinical studies and reviews have challenged this assumption, indicating that thiazide or thiazide-like diuretics may still lower blood pressure in stage 3–4 chronic kidney disease when appropriately dosed, sometimes in combination with loop diuretics [54,66–69]. Pilot studies comparing furosemide and hydrochlorothiazide in advanced chronic kidney disease further suggest that hydrochlorothiazide can contribute to blood pressure control even at reduced renal function [70,71]. Nevertheless, data remain limited at very low eGFR, and the balance between efficacy, exposure, and safety requires careful clinical assessment.

The presented PBPK/PD model has several limitations that should be considered when interpreting the results. First, data quality and reporting were heterogeneous across the included studies. Model development was constrained by the limited availability of high-quality pharmacokinetic and pharmacodynamic data in patient populations with relevant comorbidities. Although hydrochlorothiazide has been used extensively in clinical practice, systematic characterization of its disposition and effects under conditions such as cardiac, renal, or hepatic impairment remains incomplete, limiting the depth of validation in these subgroups.

Quantitative data describing the renal handling of hydrochlorothiazide, particularly tubular secretion and reabsorption processes, are sparse. Consequently, renal clearance processes were parameterized empirically rather than through fully mechanistic representations of transporter-mediated pathways. This approach is consistent with standard PBPK practice when detailed transporter kinetics are unavailable, but it introduces uncertainty when extrapolating to extreme degrees of renal dysfunction.

PBPK modeling is inherently dependent on the availability of high-quality input data, rigorous validation against experimental observations, and appropriate handling of computational complexity in large-scale simulations [72]. Future clinical and mechanistic studies, particularly in underrepresented patient populations, would support further refinement of model structure and parameterization and strengthen confidence in prospective simulations.

One study, Beermann1976 [2], reported values that were inconsistent with physiologically plausible concentration ranges and deviated substantially from the other clinical datasets. Despite extensive review, the discrepancy could not be reconciled and may reflect a unit conversion or reporting error in the original source. Accordingly, this outlier dataset was excluded from model calibration and evaluation.

Future studies should expand and harmonize clinical data for hydrochlorothiazide, particularly in patients with comorbidities. More comprehensive datasets including aligned plasma concentration–time profiles, urinary excretion data, blood pressure endpoints, and electrolyte measurements, espe-

 doi:10.20944/preprints202607.0306.v1

cially under multiple-dose conditions, would enable deeper mechanistic evaluation and strengthen model validation across organ-function strata. Impairment studies should report not only hepatic or cardiac disease status but also renal clearance, glomerular filtration rate, cardiac output or heart failure severity, and relevant markers of fluid and electrolyte balance.

Although the model performed robustly in renal impairment, additional datasets spanning a broader range of renal function would further refine the characterization of exposure–response relationships. Standardized reporting across impairment studies would enhance mechanistic interpretation and improve the predictive performance of PBPK/PD models in heterogeneous patient populations. Clinically, careful monitoring of therapeutic response, volume status, renal function, and electrolyte balance remains important in patients with cardiac, renal, or hepatic impairment receiving hydrochlorothiazide.

All model files, SBML code, simulation scripts, and curated datasets are openly accessible in accordance with FAIR principles, supporting transparency, reproducibility, independent validation, and reuse. The presented PBPK/PD model provides an extensible framework to investigate hydrochlorothiazide variability across clinically relevant conditions and supports model-informed assessment of individualized antihypertensive therapy.

Supplementary Materials: The following supporting information can be downloaded at website of this paper posted on Preprints.org.

Author Contributions: Conceptualization, A.S. and M.K.; methodology, A.S. and M.K.; software, A.S. and M.K.; validation, A.S. and M.K.; formal analysis, A.S. and M.K.; data curation, A.S. and M.K.; writing—original draft preparation, A.S. and M.K.; writing—review and editing, A.S. and M.K.; visualization, A.S. and M.K.; supervision, M.K.; project administration, M.K.; funding acquisition, M.K. All authors have read and agreed to the published version of the manuscript.

Funding: M.K. was supported by the Federal Ministry of Research, Technology and Space (BMFTR, Germany) within ATLAS by grant number 031L0304B and by the German Research Foundation (DFG) by the DFG grant number 436883643 and 465194077.

Institutional Review Board Statement: Not applicable.

Informed Consent Statement: Not applicable.

Data Availability Statement: All curated pharmacokinetic and pharmacodynamic data are publicly available in the PK-DB database (https://pk-db.com). The model and all associated materials (simulation scripts, parameters, and documentation) are publicly available in SBML format under a CC-BY 4.0 license at https://github.com/matthiaskoenig/hctz-model [39].

Acknowledgments: We acknowledge the support from Prof. Nils Blüthgen from the Charité -Universitätsmedizin Berlin. This work was supported by the BMBF-funded de.NBI Cloud within the German Network for Bioinformatics Infrastructure (de.NBI) (031A537B, 031A533A, 031A538A, 031A533B, 031A535A, 031A537C, 031A534A, 031A532B). Figures were created in BioRender. König, M. (2026) https://BioRender.com/95aly5o.

Conflicts of Interest: The authors declare no conflicts of interest.

References

1. Agboyibor, K.; Cieza, A.; Kamenov, K. Global Report on Hypertension 2025: High Stakes – Turning Evidence into Action. Technical report, World Health Organization, Geneva, 2025.
2. Beermann, B.; Groschinsky-Grind, M.; Rosén, A. Absorption, Metabolism, and Excretion of Hydrochlorothiazide. *Clin Pharmacol Ther* **1976**, *19*, 531–537. https://doi.org/10.1002/cpt1976195part1531.
3. Barbhaiya, R.H.; Craig, W.A.; Corrick-West, H.P.; Welling, P.G. Pharmacokinetics of Hydrochlorothiazide in Fasted and Nonfasted Subjects: A Comparison of Plasma Level and Urinary Excretion Methods. *J Pharm Sci* **1982**, *71*, 245–248. https://doi.org/10.1002/jps.2600710226.
4. Mylan Pharmaceuticals Inc.. FDA Approved Drug Products: Hydrochlorothiazide Oral Tablets, 2011.
5. Unichem Pharmaceuticals Inc.. FDA Approved Drug Products: Hydrochlorothiazide Capsules USP, 12.5 Mg, 2024.

 doi:10.20944/preprints202607.0306.v1

6. Chen, T.M.; Chiou, W.L. Large Differences in the Biological Half-Life and Volume of Distribution of Hydrochlorothiazide in Normal Subjects from Eleven Studies. Correlation with Their Last Blood Sampling Times. *Int J Clin Pharmacol Ther Toxicol* **1992**, *30*, 34–37.
7. Patel, R.B.; Patel, U.R.; Rogge, M.C.; Shah, V.P.; Prasad, V.K.; Selen, A.; Welling, P.G. Bioavailability of Hydrochlorothiazide from Tablets and Suspensions. *J Pharm Sci* **1984**, *73*, 359–361. https://doi.org/10.1002/jps.2600730317.
8. Beermann, B.; Groschinsky-Grind, M. Pharmacokinetics of Hydrochlorothiazide in Patients with Congestive Heart Failure. *Br J Clin Pharmacol* **1979**, *7*, 579–583. https://doi.org/10.1111/j.1365-2125.1979.tb04646.x.
9. Haas, M. The Na-K-Cl Cotransporters. *Am J Physiol* **1994**, *267*, C869–885. https://doi.org/10.1152/ajpcell.1994.267.4.C869.
10. Seely, J.F.; Dirks, J.H. Site of Action of Diuretic Drugs. *Kidney Int* **1977**, *11*, 1–8. https://doi.org/10.1038/ki.1977.1.
11. Duarte, J.D.; Cooper-DeHoff, R.M. Mechanisms for Blood Pressure Lowering and Metabolic Effects of Thiazide and Thiazide-like Diuretics. *Expert Rev Cardiovasc Ther* **2010**, *8*, 793–802. https://doi.org/10.1586/erc.10.27.
12. Preziosi, P.; Marmo, E.; Miele, E. On the Mechanism of the Anti-Hypertensive Effect of Hydrochlorothiazide. *Chemotherapia (Basel)* **1961**, *2*, 1–6. https://doi.org/10.1159/000219490.
13. Khan, M.S.; Shahid, I.; Bennis, A.; Rakisheva, A.; Metra, M.; Butler, J. Global Epidemiology of Heart Failure. *Nat Rev Cardiol* **2024**, *21*, 717–734. https://doi.org/10.1038/s41569-024-01046-6.
14. Zeng, X.; Zeng, Q.; Zhou, L.; Zhu, H.; Luo, J. Prevalence of Chronic Kidney Disease Among US Adults With Hypertension, 1999 to 2018. *Hypertension* **2023**, *80*, 2149–2158. https://doi.org/10.1161/HYPERTENSIONAHA.123.21482.
15. Ishani, A.; Hau, C.; Raju, S.; Wise, J.K.; Glassman, P.A.; Taylor, A.A.; Ferguson, R.E.; Cushman, W.C.; Leatherman, S.M. Chlorthalidone vs Hydrochlorothiazide and Kidney Outcomes in Patients With Hypertension: A Secondary Analysis of a Randomized Clinical Trial. *JAMA Netw Open* **2024**, *7*, e2449576. https://doi.org/10.1001/jamanetworkopen.2024.49576.
16. Esposito, M.; Buono, R.; Angeli, P.; Girardi, P.; Di Pascoli, M. Cardiometabolic Risk Factors and Clinical Course of Liver Cirrhosis. *Digestive and Liver Disease* **2025**, *57*, 869–876. https://doi.org/10.1016/j.dld.2024.11.021.
17. Choi, J.C.; Yoo, J.J. Hepatorenal Syndrome. *Korean J Gastroenterol* **2023**, *82*, 224–232. https://doi.org/10.4166/kjg.2023.108.
18. Westphal, J.F.; Brogard, J.M. Drug Administration in Chronic Liver Disease:. *Drug Safety* **1997**, *17*, 47–73. https://doi.org/10.2165/00002018-199717010-00004.
19. Van Wart, S.A.; Shoaf, S.E.; Mallikaarjun, S.; Mager, D.E. Population-Based Meta-Analysis of Hydrochlorothiazide Pharmacokinetics. *Biopharm Drug Dispos* **2013**, *34*, 527–539. https://doi.org/10.1002/bdd.1863.
20. Chae, J.W.; Baek, I.H.; Seo, J.W.; Jung, S.H.; Back, H.M.; Song, B.J.; Lee, B.Y.; Yun, H.Y.; Kang, W.; Kwon, K.I. Development of a Population Pharmacokinetic Model to Describe Olmesartan Medoxomil/ Hydrochlorothiazide (20/12.5 Mg) FDC Tablet in Male Healthy South Korean Subjects. *Int J Clin Pharmacol Ther* **2014**, *52*, 676–683. https://doi.org/10.5414/CP202046.
21. Commander, S.J.; Wu, H.; Boakye-Agyeman, F.; Melloni, C.; Hornik, C.D.; Zimmerman, K.; Al-Uzri, A.; Mendley, S.R.; Harper, B.; Cohen-Wolkowiez, M.; et al. Pharmacokinetics of Hydrochlorothiazide in Children: A Potential Surrogate for Renal Secretion Maturation. *J Clin Pharmacol* **2021**, *61*, 368–377. https://doi.org/10.1002/jcph.1739.
22. Rhee, S.j.; Lee, H.A.; Lee, S.; Kim, E.; Jeon, I.; Song, I.S.; Yu, K.S. Physiologically Based Pharmacokinetic Modeling of Fimasartan, Amlodipine, and Hydrochlorothiazide for the Investigation of Drug–Drug Interaction Potentials. *Pharm Res* **2018**, *35*, 236. https://doi.org/10.1007/s11095-018-2511-5.
23. Hedaya, M.A.; Helmy, S.A. Modeling of the Pharmacokinetic/Pharmacodynamic Interaction between Irbesartan and Hydrochlorothiazide in Normotensive Subjects. *Biopharm & Drug Disp* **2015**, *36*, 216–231. https://doi.org/10.1002/bdd.1935.
24. Redalieu, E.; Chan, K.K.; Tipnis, V.; Zak, S.B.; Gilleran, T.G.; Wagner, W.E.; LeSher, A.R. Kinetics of Hydrochlorothiazide Absorption in Humans. *Journal of Pharmaceutical Sciences* **1985**, *74*, 765–767. https://doi.org/10.1002/jps.2600740714.
25. Hao, K.; Chen, Y.; Zhao, X.; Liu, X. Pharmacokinetic-Pharmacodynamic Model of the Antihypertensive Interaction between Telmisartan and Hydrochlorothiazide in Spontaneously Hypertensive Rats. *J Pharm Pharmacol* **2014**, *66*, 1112–1121. https://doi.org/10.1111/jphp.12230.

 doi:10.20944/preprints202607.0306.v1

26. Snelder, N.; Ploeger, B.A.; Luttringer, O.; Rigel, D.F.; Webb, R.L.; Feldman, D.; Fu, F.; Beil, M.; Jin, L.; Stanski, D.R.; et al. PKPD Modelling of the Interrelationship between Mean Arterial BP, Cardiac Output and Total Peripheral Resistance in Conscious Rats. *Br J Pharmacol* **2013**, *169*, 1510–1524. https://doi.org/10.1111/bph.12190.
27. Yu, D.; Chen, Y.; Hao, K. The Pharmacokinetic-Pharmacodynamic Model of Telmisartan and Hydrochlorothiazide on Blood Pressure and Plasma Potassium after Long-Term Administration in Spontaneously Hypertensive Rats. *Fundam Clin Pharmacol* **2015**, *29*, 543–552. https://doi.org/10.1111/fcp.12152.
28. Gonzalez Hernandez, F.; Carter, S.J.; Iso-Sipilä, J.; Goldsmith, P.; Almousa, A.A.; Gastine, S.; Lilaonitkul, W.; Kloprogge, F.; Standing, J.F. An Automated Approach to Identify Scientific Publications Reporting Pharmacokinetic Parameters. *Wellcome Open Res* **2021**, *6*, 88. https://doi.org/10.12688/wellcomeopenres.16718.1.
29. Grzegorzewski, J.; Brandhorst, J.; Green, K.; Eleftheriadou, D.; Duport, Y.; Barthorscht, F.; Köller, A.; Ke, D.Y.J.; De Angelis, S.; König, M. PK-DB: Pharmacokinetics Database for Individualized and Stratified Computational Modeling. *Nucleic Acids Res* **2021**, *49*, D1358–D1364. https://doi.org/10.1093/nar/gkaa990.
30. Rohatgi, A. WebPlotDigitizer.
31. Hucka, M.; Bergmann, F.T.; Chaouiya, C.; Dräger, A.; Hoops, S.; Keating, S.M.; König, M.; Novère, N.L.; Myers, C.J.; Olivier, B.G.; et al. The Systems Biology Markup Language (SBML): Language Specification for Level 3 Version 2 Core Release 2. *Journal of Integrative Bioinformatics* **2019**, *16*. https://doi.org/10.1515/jib-2019-0021.
32. Keating, S.M.; Waltemath, D.; König, M.; Zhang, F.; Dräger, A.; Chaouiya, C.; Bergmann, F.T.; Finney, A.; Gillespie, C.S.; Helikar, T.; et al. SBML Level 3: An Extensible Format for the Exchange and Reuse of Biological Models. *Mol Syst Biol* **2020**, *16*, e9110. https://doi.org/10.15252/msb.20199110.
33. König, M. Sbmlutils: Python Utilities for SBML **2026**. https://doi.org/10.5281/zenodo.18207772.
34. König, M. Sbmlsim: SBML Simulation Made Easy **2026**. https://doi.org/10.5281/zenodo.18452043.
35. Somogyi, E.T.; Bouteiller, J.M.; Glazier, J.A.; König, M.; Medley, J.K.; Swat, M.H.; Sauro, H.M. libRoadRunner: A High Performance SBML Simulation and Analysis Library. *Bioinformatics* **2015**, *31*, 3315–3321. https://doi.org/10.1093/bioinformatics/btv363.
36. Welsh, C.; Xu, J.; Smith, L.; König, M.; Choi, K.; Sauro, H.M. libRoadRunner 2.0: A High Performance SBML Simulation and Analysis Library. *Bioinformatics* **2023**, *39*, btac770. https://doi.org/10.1093/bioinformatics/btac770.
37. König, M.; Dräger, A.; Holzhütter, H.G. CySBML: A Cytoscape Plugin for SBML. *Bioinformatics* **2012**, *28*, 2402–2403. https://doi.org/10.1093/bioinformatics/bts432.
38. König, M. Cy3SBML - SBML for Cytoscape **2025**. https://doi.org/10.5281/zenodo.15009089.
39. Schwaiger, A.; König, M. Physiologically Based Pharmacokinetic/Pharmacodynamic (PBPK/PD) Model of Hydrochlorothiazide. Zenodo, 2026. https://doi.org/10.5281/zenodo.20409640.
40. Stevens, P.E.; Ahmed, S.B.; Carrero, J.J.; Foster, B.; Francis, A.; Hall, R.K.; Herrington, W.G.; Hill, G.; Inker, L.A.; Kazancıoğlu, R.; et al. KDIGO 2024 Clinical Practice Guideline for the Evaluation and Management of Chronic Kidney Disease. *Kidney International* **2024**, *105*, S117–S314. https://doi.org/10.1016/j.kint.2023.10.018.
41. Köller, A.; Grzegorzewski, J.; König, M. Physiologically Based Modeling of the Effect of Physiological and Anthropometric Variability on Indocyanine Green Based Liver Function Tests. *Front. Physiol.* **2021**, *12*, 757293. https://doi.org/10.3389/fphys.2021.757293.
42. Azumaya, C.T. Sensitive Liquid Chromatographic Method for the Determination of Hydrochlorothiazide in Human Plasma. *J Chromatogr* **1990**, *532*, 168–174. https://doi.org/10.1016/s0378-4347(00)83765-2.
43. Jordö, L.; Johnsson, G.; Lundborg, P.; Persson, B.A.; Regärdh, C.G.; Rönn, O. Bioavailability and Disposition of Metoprolol and Hydrochlorothiazide Combined in One Tablet and of Separate Doses of Hydrochlorothiazide. *Br J Clin Pharmacol* **1979**, *7*, 563–567. https://doi.org/10.1111/j.1365-2125.1979.tb04643.x.
44. Anderson, K.V.; Brettell, H.R.; Aikawa, J.K. C14-Labeled Hydrochlorothiazide in Human Beings. *Arch Intern Med* **1961**, *107*, 736–742. https://doi.org/10.1001/archinte.1961.03620050102011.
45. Barbhaiya, R.H.; Patel, R.B.; Corrick-West, H.P.; Joslin, R.S.; Welling, P.G. Comparative Bioavailability and Pharmacokinetics of Hydrochlorothiazide from Oral Tablet Dosage Forms, Determined by Plasma Level and Urinary Excretion Methods. *Biopharm Drug Dispos* **1982 Oct-Dec**, *3*, 329–336. https://doi.org/10.1002/bdd.2510030406.
46. Beermann, B.; Groschinsky-Grind, M.; Lindstrom, B. Bioavailability of Two Hydrochlorothiazide Preparations. *Eur J Clin Pharmacol* **1977**, *11*, 203–205. https://doi.org/10.1007/BF00606411.

 doi:10.20944/preprints202607.0306.v1

47. Devineni, D.; Vaccaro, N.; Polidori, D.; Rusch, S.; Wajs, E. Effects of Hydrochlorothiazide on the Pharmacokinetics, Pharmacodynamics, and Tolerability of Canagliflozin, a Sodium Glucose Co-Transporter 2 Inhibitor, in Healthy Participants. *Clin Ther* **2014**, *36*, 698–710. https://doi.org/10.1016/j.clinthera.2014.02.022.
48. Giudicelli, J.F.; Richer, C.; Mattei, A. Pharmacokinetics and Biological Effects of Captopril and Hydrochlorothiazide after Acute and Chronic Administration Either Alone or in Combination in Hypertensive Patients. *Br J Clin Pharmacol* **1987**, *23 Suppl 1*, 51S–63S. https://doi.org/10.1111/j.1365-2125.1987.tb03122.x.
49. Heise, T.; Mattheus, M.; Woerle, H.J.; Broedl, U.C.; Macha, S. Assessing Pharmacokinetic Interactions between the Sodium Glucose Cotransporter 2 Inhibitor Empagliflozin and Hydrochlorothiazide or Torasemide in Patients with Type 2 Diabetes Mellitus: A Randomized, Open-Label, Crossover Study. *Clin Ther* **2015**, *37*, 793–803. https://doi.org/10.1016/j.clinthera.2014.12.018.
50. Howes, L.G.; Conway, E.L.; Phillips, P.A.; Broadbear, J.; Drummer, O.H.; Louis, W.J. Pharmacokinetic Comparison of a Combination Tablet of Enalapril and Hydrochlorothiazide with Enalapril and Hydrochlorothiazide Tablets Administered Together and Separately. *Biopharm Drug Dispos* **1991 Aug-Sep**, *12*, 447–455. https://doi.org/10.1002/bdd.2510120606.
51. Hsiao, H.L.; Langenickel, T.H.; Greeley, M.; Roberts, J.; Zhou, W.; Pal, P.; Rebello, S.; Rajman, I.; Sunkara, G. Pharmacokinetic Drug-Drug Interaction Assessment between LCZ696, an Angiotensin Receptor Neprilysin Inhibitor, and Hydrochlorothiazide, Amlodipine, or Carvedilol. *Clin Pharmacol Drug Dev* **2015**, *4*, 407–417. https://doi.org/10.1002/cpdd.183.
52. Hunninghake, D.B.; Hibbard, D.M. Influence of Time Intervals for Cholestyramine Dosing on the Absorption of Hydrochlorothiazide. *Clin Pharmacol Ther* **1986**, *39*, 329–334. https://doi.org/10.1038/clpt.1986.48.
53. Jeon, H.; Lim, K.S.; Shin, K.H.; Kim, J.; Yoon, S.H.; Cho, J.Y.; Shin, S.G.; Jang, I.J.; Yu, K.S. Assessment of the Drug-Drug Interactions between Fimasartan and Hydrochlorothiazide in Healthy Volunteers. *J Cardiovasc Pharmacol* **2012**, *59*, 84–91. https://doi.org/10.1097/FJC.0b013e318237389e.
54. Knauf, H.; Mutschler, E. Diuretic Effectiveness of Hydrochlorothiazide and Furosemide Alone and in Combination in Chronic Renal Failure:. *Journal of Cardiovascular Pharmacology* **1995**, *26*, 394–400. https://doi.org/10.1097/00005344-199509000-00008.
55. Koytchev, R.; Ozalp, Y.; Erenmemisoglu, A.; van der Meer, M.J.; Alpan, R.S. Combination of Losartan and Hydrochlorothiazide: In Vivo Bioequivalence. *Arzneimittelforschung* **2004**, *54*, 611–617. https://doi.org/10.1055/s-0031-1297058.
56. Niemeyer, C.; Hasenfuss, G.; Wais, U.; Knauf, H.; Schäfer-Korting, M.; Mutschler, E. Pharmacokinetics of Hydrochlorothiazide in Relation to Renal Function. *Eur J Clin Pharmacol* **1983**, *24*, 661–665. https://doi.org/10.1007/BF00542218.
57. Nilsen, O.G.; Sellevold, O.F.; Romfo, O.S.; Smedsrud, A.; Grynne, B.; Williams, P.E.; Kleinbloesem, C.H. Pharmacokinetics and Effects on Renal Function Following Cilazapril and Hydrochlorothiazide Alone and in Combination in Healthy Subjects and Hypertensive Patients. *Br J Clin Pharmacol* **1989**, *27 Suppl 2*, 323S–328S. https://doi.org/10.1111/j.1365-2125.1989.tb03499.x.
58. Niopas, I.; Daftsios, A.C.; Nikolaidis, N. Evaluation of the Bioequivalence of Two Tablet Formulations of Enalapril/Hydrochlorothiazide after Single Oral Administration to Healthy Volunteers. *Arzneimittelforschung* **2004**, *54*, 160–165. https://doi.org/10.1055/s-0031-1296953.
59. Ripley, E.; King, K.; Sica, D.A. Racial Differences in Response to Acute Dosing with Hydrochlorothiazide. *Am J Hypertens* **2000**, *13*, 157–164. https://doi.org/10.1016/s0895-7061(99)00168-5.
60. Vaidyanathan, S.; Valencia, J.; Kemp, C.; Zhao, C.; Yeh, C.M.; Bizot, M.N.; Denouel, J.; Dieterich, H.A.; Dole, W.P. Lack of Pharmacokinetic Interactions of Aliskiren, a Novel Direct Renin Inhibitor for the Treatment of Hypertension, with the Antihypertensives Amlodipine, Valsartan, Hydrochlorothiazide (HCTZ) and Ramipril in Healthy Volunteers. *Int J Clin Pract* **2006**, *60*, 1343–1356. https://doi.org/10.1111/j.1742-1241.2006.01164.x.
61. Weir, S.J.; Dimmitt, D.C.; Lanman, R.C.; Morrill, M.B.; Geising, D.H. Steady-State Pharmacokinetics of Diltiazem and Hydrochlorothiazide Administered Alone and in Combination. *Biopharm Drug Dispos* **1998**, *19*, 365–371. https://doi.org/10.1002/(sici)1099-081x(199809)19:6<365::aid-bdd112>3.0.co;2-r.
62. Williams, R.L.; Davies, R.O.; Berman, R.S.; Holmes, G.I.; Huber, P.; Gee, W.L.; Lin, E.T.; Benet, L.Z. Hydrochlorothiazide Pharmacokinetics and Pharmacologic Effect: The Influence of Indomethacin. *J Clin Pharmacol* **1982**, *22*, 32–41. https://doi.org/10.1002/j.1552-4604.1982.tb05705.x.
63. Koytchev, R.; Ozalp, Y.; Erenmemisoglu, A.; van der Meer, M.J.; Alpan, R.S. Effect of the Combination of Lisinopril and Hydrochlorothiazide on the Bioequivalence of Tablet Formulations. *Arzneimittelforschung* **2004**, *54*, 605–610. https://doi.org/10.1055/s-0031-1297057.

 doi:10.20944/preprints202607.0306.v1

64. Ginès, P.; Martin, P.Y.; Niederberger, M. Prognostic Significance of Renal Dysfunction in Cirrhosis. *Kidney Int Suppl* **1997**, *61*, S77–82.
65. Slack, A.; Yeoman, A.; Wendon, J. Renal Dysfunction in Chronic Liver Disease. *Crit Care* **2010**, *14*, 214. https://doi.org/10.1186/cc8855.
66. Knauf, H.; Mutschler, E. Pharmacodynamics and Pharmacokinetics of Xipamide in Patients with Normal and Impaired Kidney Function. *Eur J Clin Pharmacol* **1984**, *26*, 513–520. https://doi.org/10.1007/BF00542150.
67. Knauf, H.; Cawello, W.; Schmidt, G.; Mutschler, E. The Saluretic Effect of the Thiazide Diuretic Bemetizide in Relation to the Glomerular Filtration Rate. *Eur J Clin Pharmacol* **1994**, *46*. https://doi.org/10.1007/BF00195908.
68. Wollam, G.L.; Tarazi, R.C.; Bravo, E.L.; Dustan, H.P. Diuretic Potency of Combined Hydrochlorothiazide and Furosemide Therapy in Patients with Azotemia. *The American Journal of Medicine* **1982**, *72*, 929–938. https://doi.org/10.1016/0002-9343(82)90854-3.
69. Minutolo, R.; De Nicola, L.; Mallamaci, F.; Zoccali, C. Thiazide Diuretics Are Back in CKD: The Case of Chlorthalidone. *Clinical Kidney Journal* **2023**, *16*, 41–51. https://doi.org/10.1093/ckj/sfac198.
70. Dussol, B.; Moussi-Frances, J.; Morange, S.; Somma-Delpero, C.; Mundler, O.; Berland, Y. A Randomized Trial of Furosemide vs Hydrochlorothiazide in Patients with Chronic Renal Failure and Hypertension. *Nephrology Dialysis Transplantation* **2005**, *20*, 349–353. https://doi.org/10.1093/ndt/gfh650.
71. Dussol, B.; Moussi-Frances, J.; Morange, S.; Somma-Delpero, C.; Mundler, O.; Berland, Y. A Pilot Study Comparing Furosemide and Hydrochlorothiazide in Patients with Hypertension and Stage 4 or 5 Chronic Kidney Disease. *J Clin Hypertens (Greenwich)* **2012**, *14*, 32–37. https://doi.org/10.1111/j.1751-7176.2011.00564.x.
72. Sager, J.E.; Yu, J.; Ragueneau-Majlessi, I.; Isoherranen, N. Physiologically Based Pharmacokinetic (PBPK) Modeling and Simulation Approaches: A Systematic Review of Published Models, Applications, and Model Verification. *Drug Metabolism and Disposition* **2015**, *43*, 1823–1837. https://doi.org/10.1124/dmd.115.065920.